FAST STARTING HOLLOW CATHODES FOR SOUNDING ROCKET-BASED TETHER EXPERIMENTS

J. D. Williams, B. Rubin, and C. C. Farnell
Colorado State University
Fort Collins, CO

ABSTRACT

Data are presented on cathode temperature profiles, electron emission profiles under no-flow conditions, and timed starting tests with gas flow. Correlations between the temporal behavior of the no-flow emission current and the starting time are made, and a model is presented of the barium/barium-oxide generation and surface diffusion processes that describe the electron emission profile and starting time behavior of a hollow cathode. Future tests for evaluating effects of fast conditioning/starting sequences are described. A stand alone test pallet containing all of the sub-systems required to quickly start and operate a hollow cathode has been built and is described. The test pallet is intended for use on a sounding rocket mission and its sub-systems include gas storage and delivery, power conditioning, transducers and sensors, and an embedded micro-controller.

INTRODUCTION

Hollow cathodes have been used as plasma-based electron sources for tens of years in space applications ranging from active spacecraft potential control, electrodynamic tethers, and electric propulsion systems. In these applications, hollow cathodes have been found to be adequate in regard to emission current level, life time, heater power level, and overall reliability; however, they are not adequate in both the time required to condition them for operation (of order hours) and the time required to bring them to a temperature where they can start with ease at moderate flow rate and reasonable voltage (~3 to 6 minutes). It is especially challenging when hollow cathodes are considered for sounding rocket missions with duration of only tens of minutes.

Hollow cathode devices have been used in both orbital and sub-orbital (or sounding rocket) missions. The major difficulty in adapting the hollow cathodes for sounding rocket experiments is the problem of quickly starting the hollow cathode discharge in the limited amount of time available during the flight. In contrast to that, orbital experiments provide more time for cathode conditioning, and afford many chances to start and re-start the cathode. Some of the sounding rocket and orbital experiments where hollow cathodes have been used are described below.

In the Spacecraft Charging Sounding Rocket (SCSR) experiment conducted in January of 1978, a plasma source with a hollow cathode was used on a sounding rocket payload that was flown to an apogee of 257 km [1]. The primary purpose of this experiment was to (1) create charging on the payload by emission of both positive ions and electrons and (2) determine the relationship between environmental parameters and changes in the vehicle potential during periods of emission. The fast starting problem was solved by placing the plasma/ion source and hollow cathode within a small vacuum chamber that was pumped to low pressures prior to launch. The hollow cathode device was prepared for operation within the vacuum chamber and was pre-heated for a period of ~0.5 hr before the launch. The small vacuum chamber door was opened and the hollow cathode and ion beam system was turned “on” 103 s after launch, and the cathode was operated over a period of 340 s, from 139 km on ascent to 111 km on descent.

This effort was performed with partial support from NASA Marshall Space Flight Center under grant NNM06AA25G with oversight provided by K.L. Stephens and C. L. Johnson. Funding was also provided by Colorado State University.

Interactions between charged particles and the Earth magnetosphere were also studied in the Artificial Radiation and Aurora at Kerguelen and Soviet Union (ARAKS) experiment (1975) [2]. Specifically, high-energy electrons (in tightly focused beams) were injected into the space plasma at different pitch angles relative to the local magnetic field direction. Cesium hollow cathodes capable of 10 A fluxes were used for beam neutralization.

In the framework of the Space Power Experiment Aboard Rocket (SPEAR) program several sounding rocket experiments were carried out. The purpose of the experiments was to determine the feasibility of exposing high voltage systems to ionospheric plasma. A hollow cathode plasma contactor was used in the experiments to control the rocket potential. In the SPEAR-1 mission (conducted in 1987), the sealed cover of the contactor vacuum chamber did not come off at launch and the cathode did not operate [3]. The SPEAR-II mission was terminated because of an attitude control failure, but the SPEAR-III mission (1993) was successful in operating the hollow cathode-based plasma contactor [4].

A hollow cathode plasma contactor was used in Space Experiments with Particle Accelerators (SEPAC) onboard the Shuttle Orbiter Atlantis during the ATLAS-1 mission in 1992 [5]. This experiment utilized a hollow cathode that was placed within a 25-cm diameter discharge chamber that was capable of producing 1.5 A of xenon ions that were used to continuously neutralize a 1.5 A electron beam fired from the shuttle bay. In the Plasma Motor Generator (PMG) mission, launched to Low-Earth orbit (193 km x 869 km) in 1993, a 500-m electromagnetic tether was deployed and hollow cathodes were used to provide a low impedance bipolar electrical current between a spacecraft and the ionosphere [6]. The Thermal Ion Dynamics Experiment/ Plasma Source Instrument (TIDE/PSI) launched onboard POLAR satellite in 1996 included a hollow cathode plasma source [7]. Other notable hollow cathode plasma contactors include those used for charge control on the International Space Station [8] and on-board the DSCS-III B-7 satellite used by the Air Force to study the efficacy of plasma contactor operation for use in the elimination of differential and net charging of spacecraft in geosynchronous orbit [9].

The Propulsive Small Expendable Deployer System (ProSEDS) experimental mission also included a Hollow Cathode Plasma Contactor (HCPC) sub-system, but the ProSEDS experiment was canceled [10], and the HCPC was not flown. The HCPC utilized a hollow cathode component that required on-orbit conditioning in order to prepare it for operation (similar to many of the orbital experimental studies mentioned earlier). The total conditioning time was on the order of ten minutes, and the subsequent starting time was on the order of 150 s. Additionally, approximately 70 W of heater power was required between periods when the hollow cathode discharge was shut off during cyclic operation. This relatively large energy requirement placed stringent demands on the ProSEDS battery system, which had limited opportunities to be re-charged during the relatively long mission.

The main challenges of using a hollow cathode in a sounding rocket experiments are to (1) reduce the total energy requirements of the hollow cathode device, (2) reduce or eliminate the time required for conditioning, and (3) eliminate the need for a complicated vacuum enclosure that must be build to survive launch and then be opened after launch.

In the framework of developing a fast-starting hollow cathode, studies of hollow cathode emission characteristics have been performed under no-gas-flow conditions. Results of these tests are described herein along with measurements of the temperature of the cathode as a function of time and heater power. The data are used to verify a transient, 3D FEM thermal model and validate a coupled transient surface diffusion model that describes the migration and surface coverage fraction of low-work function material from the interior of the hollow cathode to the orifice barrel and to the exterior surface of the orifice plate of the cathode. Correlations are presented between the emission current onset and the ability to start the hollow cathode discharge once gas flow is initiated. Finally, a completely self-contained test pallet intended for sounding rockets is described that contains all of the sub-systems required to quickly start and operate a hollow cathode-based plasma contactor.

RESULTS AND DISCUSSION

The experiments on hollow cathodes described herein were performed in a Satis vacuum chamber. This vacuum chamber is pumped with a CTI Cryogenics cryopump. The operating pressure during no-gas-flow cathode experiments is 1×10^{-6} Torr. Temperatures at various locations on a hollow

cathode under test are measured using type C and K thermocouples connected to an Agilent 34970A Data Acquisition system. The cathode emission current is measured using a Keithley 6517A Programmable Electrometer.

A typical hollow cathode is shown in Fig.1. A toroidally shaped electrode is placed just downstream of the cathode, which is biased positive of the cathode to collect electrons emitted from the cathode orifice plate during testing when no gas flow is directed through the cathode.

Figure 1 *Hollow cathode test setup. The toroidal electrode located immediately downstream of the cathode orifice plate is used to measure emission current from the cathode during testing without gas flow and to initiate and sustain a discharge during testing with gas. The visual glow of the cathode corresponds to a heater current setting of 7.0 A and suggests that a significant fraction of heat loss from the cathode is due to radiation. Radiation shielding comprised of thin tantalum foil is wrapped around the cathode heater, which reduces radiation losses.*

Before a hollow cathode discharge can be started, it is necessary to prepare it for operation. This process is called conditioning and can take up to several hours for some cathodes. The purpose of conditioning is the safe removal of contaminants like water, oxygen, carbon dioxide, etc. from the low-work function insert, which is located within the hollow cathode near its downstream end. This goal is achieved by slowly increasing the cathode temperature using a swaged Ta heater while the cathode is held in a pristine vacuum environment. The heater is shown operating in Fig. 1. A 7-layer radiation shield formed from Ta foil wrapped around the heater reduces the amount of heat radiated from the cathode and increases its temperature at any given heater power level. The slow ramping of temperature is necessary because, if the cathode is heated too quickly, the insert could be "poisoned" by the out-gassing contaminants, which may not have been allowed enough time to escape from the porous structure of the insert. The pristine vacuum environment is necessary to prevent undesirable (irreversible) chemical reactions (i.e., poisoning) that can occur in poor vacuum environments containing water vapor, oxygen, and carbon dioxide at partial pressures above $1x10^{-4}$ Torr. The following conditioning sequence is used. First, the heater current through the swaged Ta heater is set to 2 A and then increased by 1 A every 5 minutes until a level of 6 A is reached. At this point, the heater current step size is reduced to 0.5 A, and two additional steps of 5-minute duration are performed at 6.5 and 7.0 A. A typical conditioning sequence is presented in Fig. 2. It is noted that conditioning can be performed with or without gas flow through the cathode, and, typically, we perform the conditioning process without gas flow. Both high purity argon and xenon gases are used for the tests described herein.

During conditioning, the emission current flowing from the cathode to the toroidal electrode (aka the keeper) is recorded. A keeper bias of +100 V relative to the cathode is applied during these measurements, and a typical emission current profile measured during conditioning is shown in Fig. 3. The emission current from the cathode begins rise (i.e., rises above zero μA) at a heater current of 6 A. This response is typical of a cathode that is equipped with (1) an insert that hasn't been operated for a significant amount of time and (2) a well-fitted heater covered with a high quality radiation shield. Cathodes that are improperly conditioned and/or poorly fitted to their heaters do not begin to emit until higher heater currents are applied. Cathodes operated at excessive temperatures or for long periods of time can also take an excessive amount of time to begin to emit. Differences between individual cathodes

can be caused by both the “condition” of the insert and the orifice plate surface properties (i.e., how well the orifice surface can be wetted by barium and barium oxide species generated by the insert). The temperature of the cathode tip as a function of heater current was also measured and is shown in Fig. 4. It is noted that higher temperatures result in higher emission current levels due to effects of both temperature and barium oxide coverage faction.

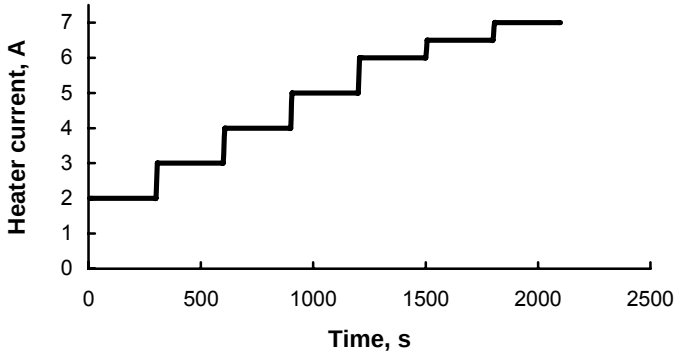

Figure 2 *Hollow cathode conditioning: Heater current vs. time.*

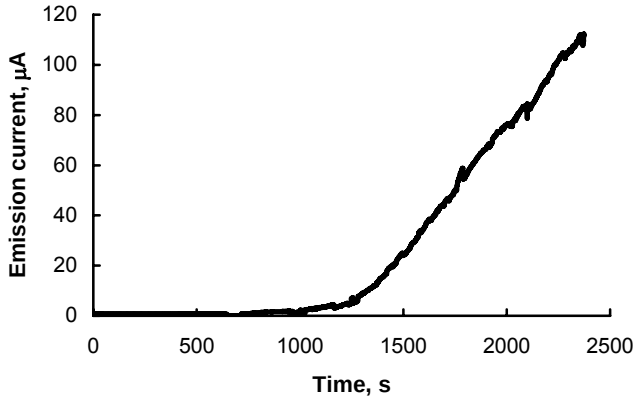

Figure 3 *Typical emission current profile during cathode conditioning.*

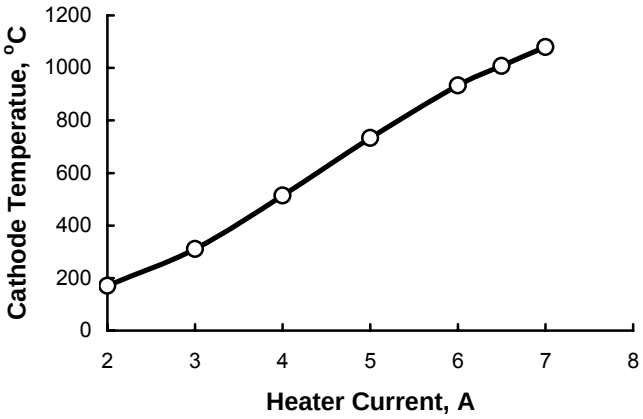

Figure 4 *Temperature vs. heater current.*

After conditioning is performed, the hollow cathode can be started (i.e., a plasma discharge can be established between the keeper and cathode). The typical requirements to start a cathode are the following: (1) Temperature of approximately 1100 ºC, (2) Gas flow in the range of 1-10 sccm, and (3) Keeper potential biases in the range of 100 to 200 V. A final requirement for starting is for the insert to coat the hollow cathode orifice barrel and orifice plate exterior with a partial mono-layer of barium oxide. The time required for the no-flow, electron emission currents to rise above 10 μA has been found to be necessary to easily start a cathode. A plot of the emission current as a function of time is shown in Fig. 5. This plot was obtained by setting the heater current to 7.0 A at t=0 sec. The time for the emission current to rise above 10 μA was observed to be ~200 sec, which is typical for most conventional orificed hollow cathodes equipped with porous tungsten inserts that are impregnated with a barium compound. As noted above, the saturation current is a function of temperature and barium-oxide surface coverage.

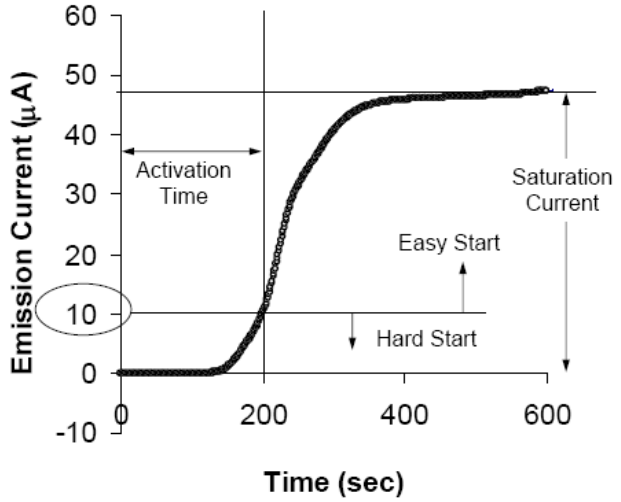

Figure 5 *Emission current profile during cathode heat-up*

Cathode activation (i.e., starting) depends on the condition of the insert, which depends on the amount of chemically available barium remaining in the insert. This amount, in turn, depends on the age of the insert where aging can be caused by excessive temperatures, excessive operational time, exposure to contaminates, and/or poor conditioning practice. As the age of an insert increases, the barium is depleted, and the time required for starting the cathode increases. Eventually the amount of chemically available barium in the insert will fall below the level required to start the cathode. To check the condition (i.e., the health) of a cathode at a given point in its history, the cathode heater is turned on (usually at a nominal level of 7 A) when the cathode is initially at room temperature. The emission current profile is then recorded as the cathode heats up (with the keeper biased relative to the cathode set at +100 V). Typical data measured during a health check are shown in Fig. 6 for three different heater power levels, and, as expected, higher heater power levels cause emission to start sooner and reach higher saturation values. As noted above, the saturation value is dependent upon both the cathode temperature and the surface coverage fraction of barium oxide on the exterior of the cathode orifice plate. The drop in emission current in Fig. 6 between 400 s and 700 s for the 7.0 A heater current condition was caused by an out-of-current regulation problem on the heater power supply where the heater current dropped below 7.0 A during this time.

In the tests described above, the temperature of the cathode tip was measured using type C thermocouples and with an optical pyrometer. The desired temperature of the cathode at startup is approximately 1100 ºC and this temperature (and the temperature profile) affects electron emission capability and drives the production of barium oxide. Therefore an understanding of the heat flow processes in the cathode is of great importance for the design of a fast-starting cathode. Figure 7 shows the temperature profiles of a cathode orifice plate during the no-flow electron emission tests corresponding to Fig. 6. Note that the time axis is expanded on Fig. 7 to provide more detail on the temperature rise near the start of the test. Also note that the emission current in Fig. 6 is plotted on a log

scale to highlight the point where the electron emission current begins to rise and to allow comparisons between the three heater current levels that were selected.

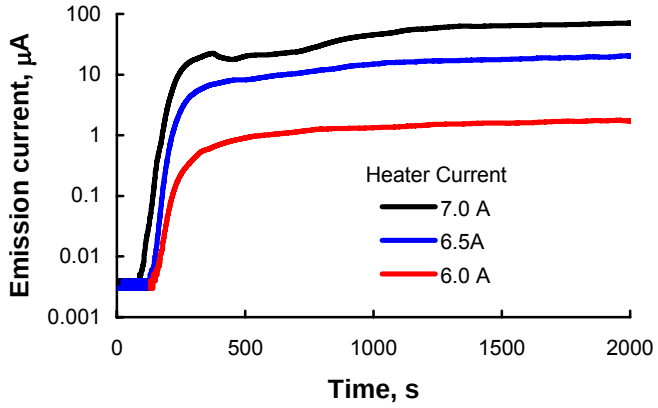

Figure 6 *Emission current vs. time for different heater current levels.*

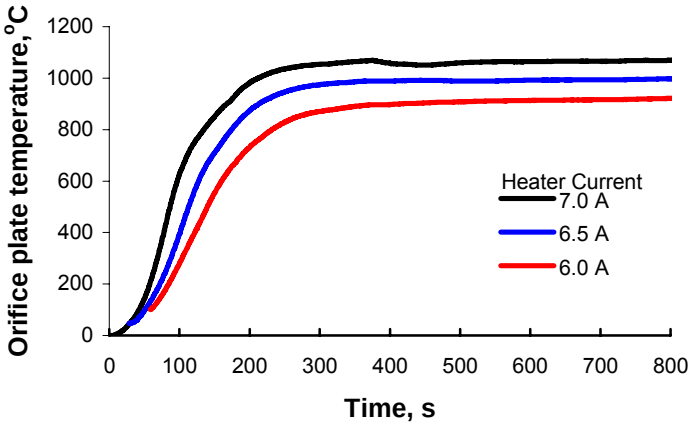

Figure 7 *Temperature vs. time for different heater current levels*

The results presented in Figs. 5, 6, and 7 are useful for verification of computational models of the cathode start-up process. A model is currently under development at CSU (that is based on the work of Tighe et al. [11]) where the temporal surface diffusion characteristics of barium oxide is modeled along with the barium oxide generation rate and the cathode/insert temperatures. The cathode start-up sequence begins with applying current to the heater that causes the cathode temperature to increase, eventually reaching approximately 1100 ºC. As the cathode heats up, barium evaporates from the cathode insert, creating a gas inside the cathode tube, which covers the inner surfaces of the cathode. The barium deposited on the interior surface of the orifice plate and within the orifice barrel diffuses to the outer surface of the orifice plate, creating a low work function emitter. This barium diffusion process is described by the surface diffusion equation:

$$D\nabla^2\theta = \frac{\partial\theta}{\partial t} + \frac{\theta}{\tau} \quad . \qquad (1)$$

In Eq. (1), D represents the surface diffusion coefficient, θ the surface coverage fraction, t the time and τ the barium desorption (or residence) time.

The boundary condition for the surface diffusion equation is the surface coverage of the orifice barrel walls. According to Longo [12], Forman [13], and Jensen [14], the coverage thickness is limited to a monolayer. At the present stage of our modeling effort, this condition was selected to fit experimental data, however, Tighe et al [11] used a Knudsen flow model as well as hollow cathode life test data to calculate the surface coverage of the barrel region from the internal pressure of the barium gas, and we plan to add this additional level of complexity to our model in the near future.

After the surface coverage is determined, the work function φ over the exterior of the orifice plate can be determined using the equation derived by Longo [12]:

$$\phi(\theta) = \varphi_W \left(\frac{\Gamma \varphi_W}{\varphi_{Ba}} \right)^{\frac{\Gamma\theta}{1-\Gamma}} + \varphi_{Ba} \left[1 - \left(\frac{\Gamma \varphi_W}{\varphi_{Ba}} \right)^{\frac{\theta}{1-\Gamma}} \right] \quad . \qquad (2)$$

In Eq. (2), Γ represents the parameter that determines the minimum work function at monolayer coverage determined from Longo's data [12], φ_W the tungsten work function, and φ_{Ba} the barium work function.

With the use of Eq. (2), we can calculate the emission current density j using the Richardson-Dushman equation combined with the Schottky term.

$$j = AT^2 e^{-\frac{q\varphi(\theta)}{kT}} e^{\frac{0.44}{T}\sqrt{\frac{V}{d}}} \qquad (3)$$

In Eq. (3), T represents the temperature of emitting surface (orifice plate), k the Boltzmann constant, V the bias voltage between the cathode and the keeper electrode, and d the distance between the cathode and the keeper electrode. This equation describes the field-enhanced, thermal emission from the exterior surface of the orifice plate. Integrating the current density over the orifice plate surface yields the emission current:

$$i = 2\pi \int_{r_1}^{r_2} j(\varphi) r dr \quad . \qquad (4)$$

At the present time, the emission current behavior is being estimated using the experimentally measured orifice plate temperature and by selecting the surface coverage boundary condition at the orifice barrel to fit the emission profile. A thermal model is also being developed (see discussion below), and, after it is validated, temperatures calculated from the thermal model can be used in place of the measured temperature profile data. The emission current profile calculated using the model described above and the experimentally measured temperature profile is presented in Fig. 8, where excellent agreement is observed with measurements of the emission current profile.

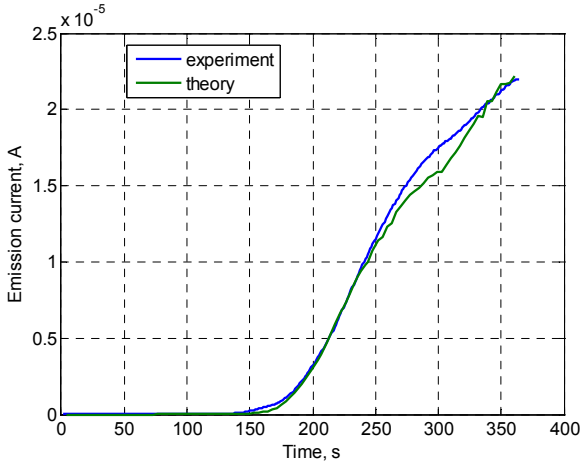

Figure 8 *Comparison of calculated and measured emission current.*

A 3-D, transient thermal model of a hollow cathode was assembled using ePhysics software from Ansoft [15]. Both conduction and radiation processes are included along with a temporal description of the power delivered to the heater. Preliminary steady-state results are shown in Fig. 10 for a heater current of 7 A. The cathode/heater coil region is shown without the radiation shield to display more information. We are currently working on improving the description of the radiation shield and how the heater power varies with time. Our plan is to compare the thermal model predictions to experimentally measured temperature profiles once these improvements are implemented.

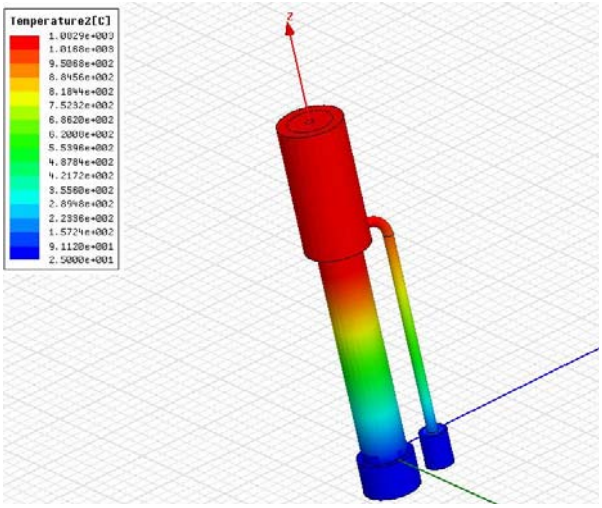

Figure 9 *Calculated steady-state temperature distribution for a heater current of 7 A.*

A tether experiment is planned by the Japanese Space Agency (JAXA) on a sounding rocket [16, 17].The goal is to test the theory of orbit-limited-motion collection of electrons on a positively-biased, bare, conducting tether in the Earth's ionosphere. Applications that will benefit from the data collected are electrodynamic tether systems planned for use in low Earth orbit for removal of orbital debris, satellite re-positioning, power generation, science investigations, and related tasks.

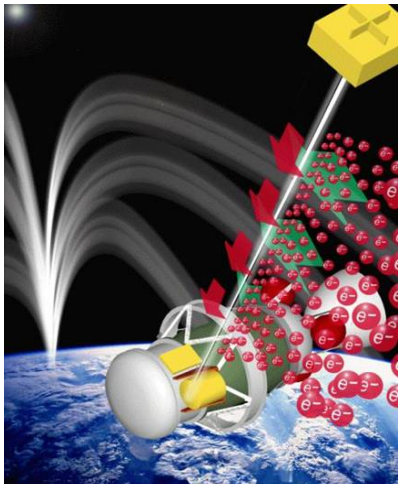

Figure 10 *An electrodynamic tether shown de-orbiting a LEO satellite. (Satellite motion is to the right.) Figure Credit: NASA Marshall Space Flight Center*

An electromagnetic tether consists of a long conducting wire deployed from a satellite in a gravity-gradient orientation with the tether either above or below the satellite. When a satellite with a metallic tether orbits around the Earth or another planet with a significant magnetosphere, the tether crosses

magnetic field lines and a voltage is generated between the ends of the tether as shown in Figure 10. If the electrical circuit is closed, an electrical current will be induced in the tether. The circuit can be closed through contact with the natural space plasma environment by collecting free electrons from the plasma at one end of a bare tether and expelling them back into plasma at the other end of the tether.

While the positively charged end of a bare tether will readily collect elections from the space plasma, the electron emission at the negatively charged end of the tether is more difficult to achieve in a passive manner. An active electron emitter, such as a hollow cathode, however, can be used for this purpose. The current in the tether will, in turn, interact with the magnetic field and produce a force that will either slow down the orbital motion of the tether and the satellite attached to it or speed up the orbital motion depending upon (1) the relative velocity of the magnetic field relative to the tether/satellite system and (2) the direction of current flow in the tether. Consequently both generator and motor modes of operation are possible.

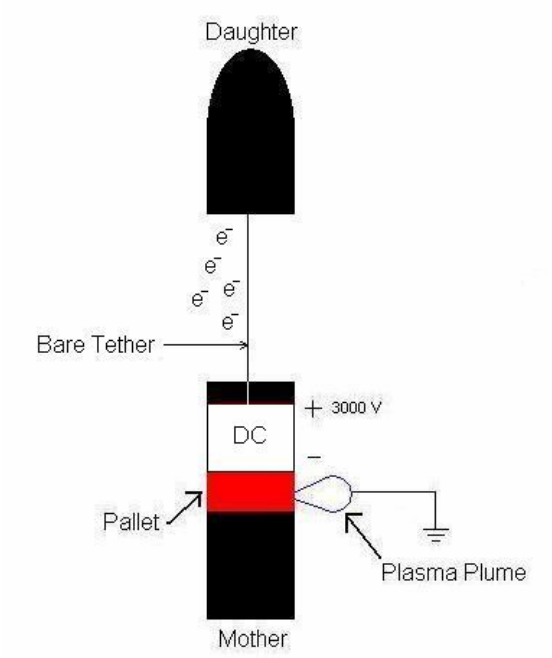

Figure 11 *Schematic of bare electromagnetic tether experiment planned by JAXA.*

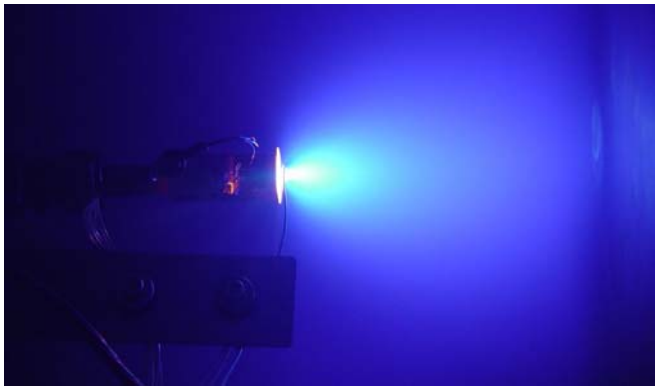

Figure 12 *Photograph of a hollow-cathode-based plasma contactor emitting electrons.*

In the generator mode of operation, the kinetic energy of orbital motion is converted into electrical energy that can be used to operate electrical loads on the spacecraft. In the motor mode of operation, a power supply is used to overcome the motion-induced emf and drive a current in a direction opposite to

the direction of normally induced current flow. The resulting force will boost the orbit of the spacecraft in a low Earth orbital environment. The unique advantage of this technique compared to other space propulsion systems is that it doesn't require any propellant other than the small amount of gas used by the hollow cathode plasma emitter. A hollow cathode is shown operating in Figure 12 where it is being used to emit ~40 A of electrons into a low pressure vacuum environment.

As a consequence of passive electron collection on a bare tether and efficient electron emission from a hollow cathode-based plasma contactor, electrodynamic tether systems can provide nearly propellant-less propulsion, dramatically reducing costs of high delta-V space missions, such as formation flying, low-altitude stationkeeping, orbit raising, and end-of-mission de-orbit operations. Recent electrodynamic tether application studies include periodic re-boosting of the International Space Station, removal of orbital debris from low Earth orbit, and scientific missions to Jupiter to name a few.

Selection of electrodynamic tether systems for difficult missions and the details of the tether design rest on the validation of OML theory and how LEO plasma conditions and orbital parameters affect the predictions of this theory. The sounding rocket experiment planned by JAXA requires a plasma device (a plasma contactor) to produce a low impedance connection between the space plasma and the mother payload end of the tether. The electrical connection to the space plasma will allow electrical biases to be applied to the tether enabling the investigation of electron collection on the tether versus bias.

Due to the short time duration of the sounding rocket mission, the plasma contactor will need to become operational within 180 seconds after launch using a minimal amount of electrical power. It is noted that conventional power efficient plasma devices can sometimes require tens of minutes or more to become operational—times that are longer than typical sounding rocket flights of six to ten minutes.

The goal of the plasma contactor system development effort described herein is to design, analyze, and fabricate all of the sub-systems and ground-support equipment that are required to quickly start and operate a plasma contactor. In addition, this task includes integration of the sub-systems into a system that is self-contained, autonomous, and straightforward to mate to the sounding rocket payload. Critical supporting sub-systems include gas storage and delivery, power conditioning and delivery, transducers and sensors, and a micro-controller. Conceptual views of a plasma contactor system are shown in Fig. 13, and a photograph of a prototype system built at CSU is shown in Fig. 14.

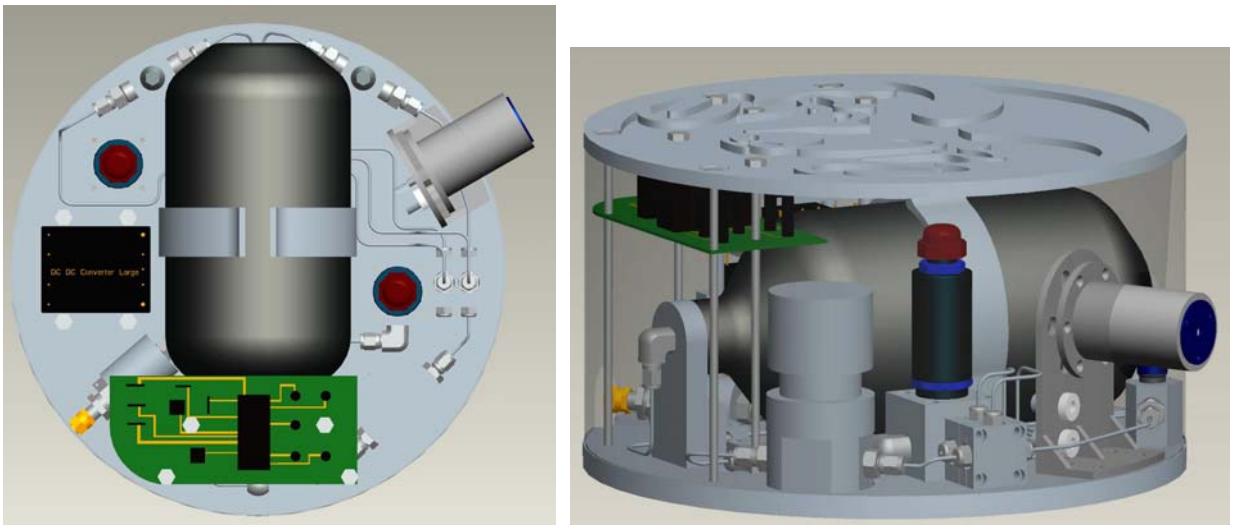

Figure 13 *Conceptual layout of a fully self-contained plasma contactor system.*

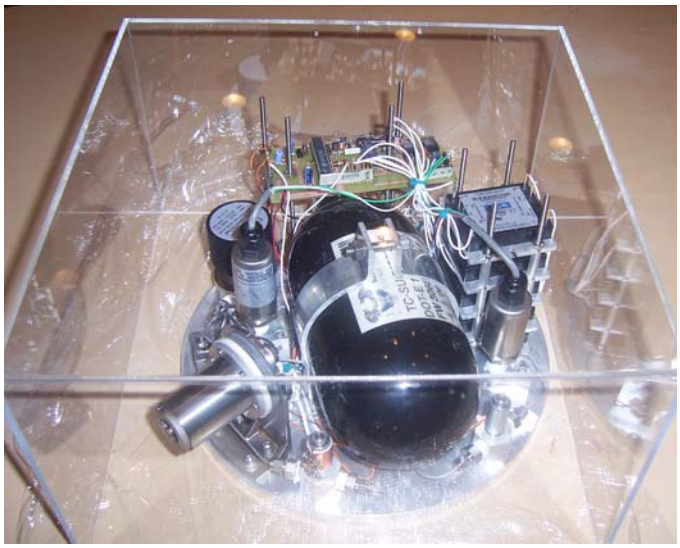

Figure 14 *Prototype plasma contactor system built at CSU shown without the enclosure.*

Critical supporting sub-systems include gas storage and delivery, power conditioning, transducers and sensors, and a micro-controller as called out in the sketch in Fig. 15.

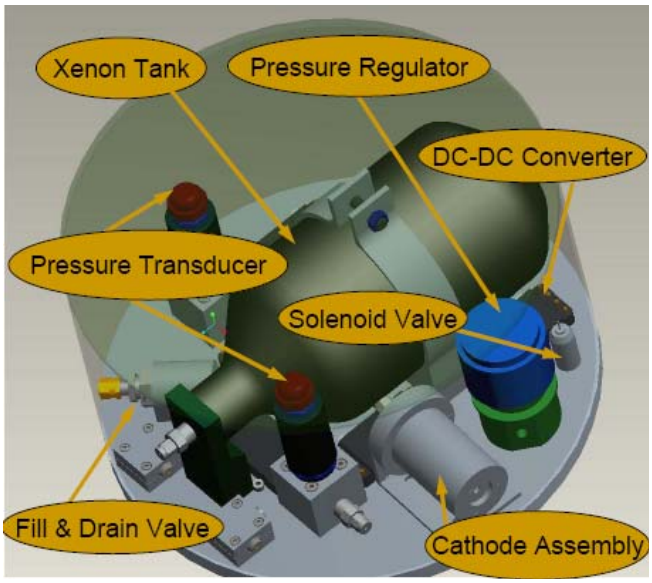

Figure 15 *Plasma contactor system layout. Note that gas lines and wiring have been omitted for clarity and the top plate and sidewall are shown semi- transparent.*

The gas delivery sub-system consists of several components including a fill and drain valve that is accessible from the outside of the test pallet. This component is used in ground support operations to fill a gas tank with high purity xenon gas prior to launch. The fill and drain valve is connected to a manifold where the gas tank is attached. Also attached to the manifold is a high-pressure transducer. Xenon gas is feed from the manifold to a latch valve and then to a pressure-reducing regulator. A solenoid valve is placed downstream of the regulator along with a flow-restricting element. Tubing is used to connect the flow restrictor to the hollow cathode. An additional pressure transducer is used to autonomously

determine when the atmospheric pressure is reduced to the point where gas purging operations can be performed prior to initiating start up of the hollow cathode. All of the gas delivery component operation and monitoring is performed by a microcontroller embedded within an electronics sub-assembly. DC-to-DC converters are used to operate the solenoid valves and provide power to the microcontroller, transducers, and sensors.

The electronics sub-system includes connectors for Ground Support Equipment (GSE) access to the test pallet. Separate DC-to-DC converters are used to provide power to the heater and plasma ignition elements of the plasma device, which are turned "on" and "off" with the micro-controller. A pulse-width modulation approach is used to control heater power application and the accelerated conditioning process. The approximate sequence of the FAST pallet system activation process is presented in Table 1.

Table 1 *Preliminary test sequence.*

Time	Operation
Several minutes prior to launch	Start purging cathode with xenon flow
Several minutes prior to launch	Start low power cathode heating
After the launch	Wait for the pressure transducer signal indicating that the atmospheric pressure is reduced to a given level
After the pressure transducer signal is received	Start gas purging, ramp-up heater power
About two minutes after the launch	Activate the cathode

SUMMARY AND CONCLUSIONS

Our paper presented data on cathode temperature profiles and electron emission profiles measured under no-flow conditions. In addition, a model was presented of the barium/barium-oxide generation and surface diffusion process that describes the electron emission temporal profile and starting time behavior. Predictions from the model were compared to experimental results and were found to be in reasonable agreement. A stand alone test pallet containing all of the sub-systems required to quickly start and operate a hollow cathode has been built and is described. The test pallet is intended for use on a sounding rocket mission and its sub-systems include gas storage and delivery, power conditioning, transducers and sensors, and an embedded micro-controller.

REFERENCES

1. H.A. Cohen, E.G. Mullen, W.B. Huber, and T. Masek, "The Sounding Rocket Flight of a Satellite Positive Ion Beam System", AIAA-1979-2068 , *14th International Electric Propulsion Conference*, Princeton, N.J., Oct. 30-Nov 1, 1979.
2. G.A. Gusev, Y.V. Kushnerevsky, S.A. Pulinets, V.V. Selegey, "Wave Phenomena Under Injection of Energetic Electrons into the Ionosphere in ARAKS Experiment", *Physics of the Ionosphere and Magnetosphere*, Nauka Publ., Moscow, 1978, p.134-143.
3. G.A. Jongeward, "Spacecraft Charging in the Spear I", *International Conference in Spacecraft Charging*, Livorno, Italy, Sept. 1991.

4. P. Rustan, H. Garrett, and M.J. Schor, **"**High Voltages in Space: Innovation in Space Insulation," IEEE Transactions on Electrical Insulation Vol. 28 No. 5, Oct. 1993, p. 855-865.
5. W.L. Taylor, S.L. Moses, T. Neubert, and S. Raganatan, "Beam Plasma Interactions Stimulated by SEPAC on - ATLAS 1: Wave Observations", *XXIVth General Assembly of the International Union of Radio Science*, Kyoto, Japan, August 25-September 2, 1993.
6. J. McCoy, et al., "Plasma Motor-Generator (PMG) Flight Results," *Proceedings of the Fourth International Conference On Tethers In Space*, Science and Technology Corp., Hampton, VA, Apr. 1995, p. 57-82.
7. T.E. Moore, C.R. Chappell, M.O. Chandler, et al., "The Thermal Ion Dynamics Experiment and Plasma Source Instrument", *Space Science Reviews*, v. 71, 1995, p. 409-458.
8. C.B. Carpenter, "On the Operational Status of the ISS Plasma Contactor Hollow Cathodes", 40th AIAA/ASME/SAE/ASEE Joint Propulsion Conference and Exhibit, 11 - 14 July 2004, Fort Lauderdale, Florida, AIAA 2004-3425.
9. L.H. Krause, D.L. Cooke, and C.L. Enloe, "Survey of DSCS-III B-7 Differential Surface Charging", *IEEE Transactions on Nuclear Science*, Dec. 2004, Vol. 51, Issue 6, Part 2, p. 3399- 3407.
10. J.A. Vaughn, L. Curtis, B.E. Gilchrist, et al, "Review of the ProSEDS Electrodynamic Tether Mission Development", 40th AIAA/ASME/SAE/ASEE Joint Propulsion Conference and Exhibit, 11 - 14 July 2004, Fort Lauderdale, Florida, AIAA-2004-3501.
11. W.G. Tighe, K. Chien, D.M. Goebel, and R.T. Longo, "Hollow Cathode Ignition Studies and Model Development," 29th International Electric Propulsion Conference, Oct. 31 – Nov. 4, 2005, IEPC-2005-314.
12. R.T. Longo, "Physics of Thermionic Dispenser Cathode Aging", *Journal of Applied Physics*, vol. 94, pp. 6966, 2003.
13. R. Forman, "Surface Studies of Barium and Barium Oxide on Tungsten and its Application to Understanding the Mechanism of Operation of an Impregnated Tungsten Cathode", *Journal of Applied Physics*, vol.47, p.5272, 1976
14. K.L. Jensen, Y.Y. Lau, and B. Levush, "Migration and Escape of Barium Atoms in a Thermionic Cathode," *IEEE Transactions on Plasma Science*, vol.29, p.772, 2000.
15. Ansoft Corporation, ePhysics™ Coupled Thermal and Stress Analysis for Electromagnetic Applications, http://www.ansoft.com/
16. H.A. Fujii, H. Takegahara, K. Oyama et al, "A Proposed Bare-Tether Experiment On Board a Sounding Rocket", 2nd International Energy Conversion Conference, Aug. 16-19, 2004, AIAA-2004-5718.
17. Personal communication with Prof. H. Fujii, Toyko Metro. Inst. of Tech, April 2007.